UNIQUENESS OF BLUR MEASURE

Jérôme BUZZI[*] *and Frédéric GUICHARD*

DXOLabs
3, rue Nationale - 92100 Boulogne - FRANCE
jbuzzi@dxo.com, fguichard@dxo.com

ABSTRACT

After discussing usual approaches to measuring blur of optical chains, we show theoretically that there is essentially a unique way to quantify blur by a single number. It is the second derivative at the origin of the Fourier transform of the kernel. This somewhat surprisingly implies that blur is especially sensitive to attenuation of the *low* frequencies. The blur measure is in fact the quadratic size of the spot diagram. A series of experiments show that this measure is correlated to perceptual blur. We verify that the blur measure behaves as expected with respect to the standard "blur" and "sharpen" tools of usual image processing tools. We apply the measure to assess quality of cameras, natural images and image processings.

Keywords: Image analysis, image quality, blur, uniqueness.

1. INTRODUCTION

The blurring produced by an imaging chain, be it a camera, a screen or an image processing algorithm, is a key component of its quality. We note that perceptual blur is a loosely defined concept (which may cover multiple and complicated psychophysical phenomena) which has been studied before mainly as "the effect of a Gaussian filter" (see, e.g., [2, 14, 27]). In this paper we ask a different question. We look for a way to quantify (non-necessarily Gaussian) "bluriness" as it is produced by various imaging chains (i) by a single number so that one can compare imaging chains; which is (ii) correlated to the perceived level of blur; (iii) can be composed in the sense that concatenating imaging chains results in a blur which a function of the blurs of the imaging chains, e.g., the blur of a camera should be a function of the blur of its optics, its sensor and the following processing. We note that this work does not deal with the blur of images *per se* (see [9] and the references therein).

In the spirit of the approach of [1] to scale-space PDE (see [11, 12, 29]), we derive mathematically a unique solution to this problem and then study how it relates to perception and apply it to imaging problems.

Blur is often measured in the two following way. The first one is the **Modulation Transfer Function** or MTF (see, e.g., [22]):

$$\mathrm{MTF}(\omega) = \frac{\int |\hat{f}_0(\omega\cos\theta, \omega\sin\theta)|\, d\theta}{\int |\hat{f}(\omega\cos\theta, \omega\sin\theta)|\, d\theta}$$

where $\hat{f}_0$ is the Fourier transform of the true image and $\hat{f}$ is that of the observed image. A perfect imaging chain would have $\mathrm{MTF}(\omega) \equiv 1$, but real imaging chains attenuate high frequencies so that $\mathrm{MTF}(\omega) \to 0$ as $\omega \to \infty$. Figure 1 shows a typical MTF. The MTF can be evaluated by measuring the response to a black-on-white edge, like the ones found in the ISO 12233 test chart [21].

The MTF seems to contain all the relevant information (it forgets the possible non-isotropy of the imaging chain and the phase of the underlying kernel —see below). Also, the MTF of a concatenation of chains is the product of their MTFs. However it is a whole function where one would like a single number and it contains lots of information irrelevant to blur.

Remark. The **spot diagram** is the image of an ideal point. A perfect optical chain would reproduce a single point. A real one gives a spot which can have a variety of shape, size and colors. The spot diagram is ideally the image of the underlying kernel. Such diagrams are much used in optics [22]. As they are theoretically very close to MTFs, the same comments apply to them.

It is a common practice to try to extract a representative number from the MTF. This is done by looking at its values at some definite frequencies (for instance Canon[1], resp. Olympus[2], recommends using the value of the MTF at 30 lp/mm, resp. 60 lp/mm, on the 24x36mm film to assess

[*] From C.N.R.S. U.M.R. 7640 & Ecole polytechnique, Palaiseau, FRANCE.

[1] See the glossary at http://consumer.usa.canon.com.

[2] See the MTF charts at http://www.olympus-pro.com.

the "sharpness", whereas the value at 10 lp/mm, resp. 20 lp/mm, should give the "contrast capability"). There is an obvious arbitrariness involved in these choices.

There are other ways to extract a number: taking the area under the MTF curve or looking at the frequency where the MTF drops below some high treshold, e.g. 75%.

Another related number is the **limiting resolution** (see, e.g., [22]). It is the size of the smallest visible details or, in other terms, the highest spatial frequency visible in the produced image. It can be measured from the MTF by declaring it to be the frequency where the MTF falls below a low threshold like 5%.

In these ways, one obtains numbers with a clear meaning. However, knowing such numbers for different optical chains does not allow one to predict the corresponding numbers for their concatenation (which can describe the zooming or printing required to actually use the images).

There is therefore a need for a better way to quantify blur with respect to the evaluation of imaging chain quality. To provide an answer we axiomatize the problem to analyze it mathematically: an imaging chain is given by its kernel K and the corresponding blur $\mathcal{B}(K)$ satisfies:

- the blur of a Gaussian kernel is non-zero;
- the blur of a concatenation of optical chains is a function of the blur of each of the chains (and does not depend on any other characteristics of these chains);
- the blur is not affected by displacements within the plane of the image: if I is an isometry of the plane, then $\mathcal{B}(K \circ I) = \mathcal{B}(K)$ for any kernel K;
- the blur observed from a distance d' is a function of the blur at a distance d and the ratio d'/d.

(A precise statement of these axioms and a more detailed discussion is given in Section 3). For now, let us comment the last axiom. It is clear that the perceived blur of an image, say a given print, depends on the distance at which it is observed. The axiom requires that there exists a function F

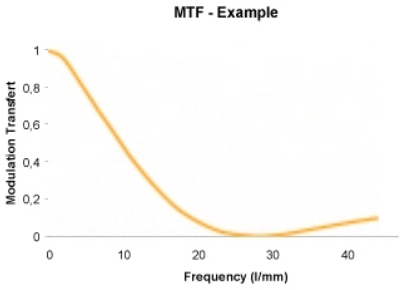

Fig. 1. A typical MTF is close to 1 for $\omega \approx 0$ and then falls off rapidly.

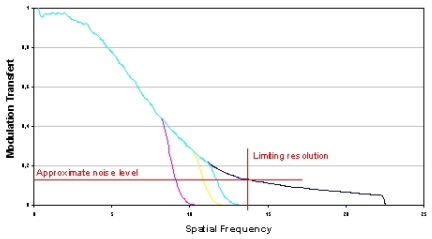

Fig. 2. MTF's differing only for large ω.

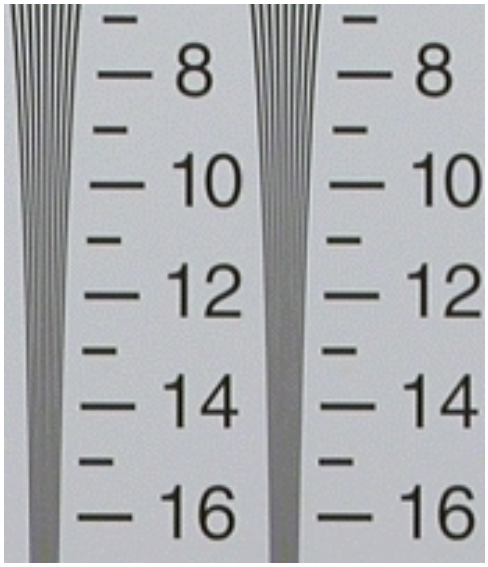

Fig. 3. Same perceptual blur with different limiting resolutions.

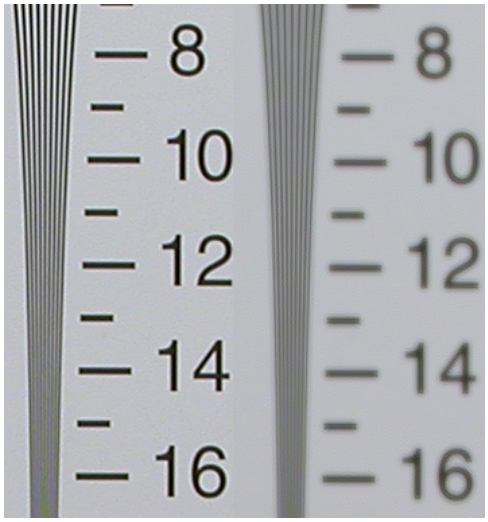

Fig. 4. Different perceptual blurrings with the same limiting resolution (ISO-12233 chart, detail).

such that the blur observed at the distance d' is $F(d/d', b)$ where b is the blur as observed at the distance d.

We obtain the following result (stated more precisely in section 3):

Theorem 1 *Any blur measure with the properties above can be written as $\Psi(\mathcal{B}(K))$ where K is the normalized kernel of the imaging chain, $\Psi : [0, \infty) \to [0, \infty)$ is a fixed, increasing diffeomorphism and*

$$\mathcal{B}(K) = -\frac{1}{2} \operatorname{tr} \frac{\partial^2 \log \hat{K}}{\partial x^2}(0, 0)$$

where $\hat{K}$ is the Fourier transform of the kernel of the optical chain and tr *is the trace. Moreover, $\mathcal{B}$ is the only blur measure which has the following additional properties:*

- *it is additive: $\mathcal{B}(K * L) = \mathcal{B}(K) + \mathcal{B}(L)$;*
- *it is* 1 *for the Gaussian kernel with variance* 1.

For a Gaussian kernel $K(x, y) = (2\pi\sigma)^{-1} e^{-(x^2+y^2)/2\sigma^2}$, $\mathcal{B}(K)$ is simply its usual parameter σ^2, as one could expect. This shows in what sense Gaussian blur can represent arbitrary blur as it is often assumed in the literature. More interestingly, this formula gives, for arbitrary kernels, the relevant generalization of the parameter σ^2.

Remark that the blur measure is therefore determined by the behavior of the kernel at vanishing frequencies: contrarily to a widespread belief (see, e.g., [19, 17]), blur is not primarily related to high frequency attenuation or low pass filters

We can already make a few comments. Firstly, it is well-known that the contrast sensitivity of the human visual system is rather low at high frequencies, hence it is perhaps not so surprising that these do not play such a big role in the overall quality of an image. Secondly, as Figures 2-4 show, one can have MTFs with the same behavior at high frequencies (in particular the same limiting resolutions) and yet very different perceptual levels of blur and conversely. Thirdly, this derivative in the Fourier domain has a simple interpretation in space and one can reformulate the previous theorem as:

Theorem 2 *The above blur measure for an optical chain given by a normalized kernel K is*

$$\mathcal{B}(K) = \frac{1}{2} \int_{\mathbb{R}^2} (x^2 + y^2) K(x, y)\, dxdy.$$

In particular, it is obviously related to the size of the spot diagram which is very natural.

The proof of these results is given in Section 4. We apply various kernels to confirm that low frequencies indeed play the dominant role in the perception of blur (section 5). We show that this mathematically defined measure is related to perception by a psychophysical experiment (section 6) which confirms the view of practitioners (mass retailers, journalists) which have adopted this measure. Then we explain how these mathematical results can be used, giving a detailed example of the assessment of cameras with given optics, print format and viewing conditions (section 7). We finally present two applications to digital image processing: we evaluate a family of linear zooms and we show how *both blur and noise* can be reduced at the price of "texturing" (section 8) before concluding.

A short version of this work was presented at [6].

2. AXIOMATICS OF BLUR MEASURES

2.1. Imaging chains and convolutions

An imaging chain is some collection of devices which takes on input an image (assumed to be some positive function on the plane) and outputs another image. We assume the imaging chains in this paper to be:

(1) positive;

(2) linear;

(3) translation invariant;

(4) L^1 norm preserving.

These assumptions can be justified as follows.

(1) Images are nonnegative functions, so imaging chains map nonnegative functions to nonnegative functions: this is the definition of positivity.

(2) Optical devices are certainly linear. Films or CCD detectors are often non-linear in theory but one usually tries to use them in their linear regimes.

(3) The situation with respect to translation invariance is similar: it rarely holds perfectly (for instance there is often vignetting), but one usually strives to approach it.

(4) The L^1 norm is the integral of the intensity and therefore the physical energy [4]. By this normalization we make the measure independent of global gain[3].

Properties (2)-(4) are well-known [5, p. 72] to imply that imaging chains correspond to convolutions, i.e., imaging chains correspond mathematically to the following operations on images f:

$$f \mapsto K * f$$

with a kernel K which is a L^1 nonnegative function over the plane. Notice that K is essentially the spot diagram in terms

[3] Such a global gain may well have a perceptual impact but this is not the subject of this paper.

of optics. The energy normalization is obtained by dividing K by its L^1 norm.

The transform of a point through an imaging chain is expected to have essentially a finite size. Thus we can assume that the kernel has finite moments of all orders.

We also assume for convenience the normalizations:

$$\int xK\,dxdy = \int yK\,dxdy = 0 \tag{1}$$

These conditions can be ensured just by translating the kernel K.

We let $\mathcal{K}$ be the set of kernels, i.e. all nonnegative, L^1 functions, with finite second order moments and satisfying the normalization (1).

We denote the Gaussian kernels by

$$G_{\sigma^2_{xx},\sigma^2_{yy}}(x,y) := \frac{1}{2\pi\sigma_{xx}\sigma_{yy}} e^{-x^2/2\sigma^2_{xx} - y^2/2\sigma^2_{yy}}$$

and simplify G_{σ^2,σ^2} to G_{σ^2}.

2.2. Blur measures

We formalize the axiomatics given informally in Section 1. Let us stress that, at this point, we are looking for a *useful quantification of blur*, not a psychophysical model of human perception. We shall discuss later evidence of a correlation.

2.2.1. Additivity

The main requirement on blur measure is that the blur of a concatenation of imaging chains is the "composition" of the blurs of the imaging chains in the following sense. There is a continuous group law $\circ$ on an interval $I \subset \mathbb{R}$ such that

$$\mathcal{B}(K * L) = \mathcal{B}(K) \circ \mathcal{B}(L)$$

But this readily implies that there is a diffeomorphism $\Psi : I \to \mathbb{R}$ such that $\Psi(x \circ y) = x + y$. Hence, up to the change of coordinates Ψ, the composition property implies that the measure is additive.

2.2.2. Rescaling

The second requirement is the covariance w.r.t. change of scale or distance of observation: there is a continuous $(z,b) \mapsto F_z(b)$ such that, if z is some zooming factor, then $\mathcal{B}(K^z) = F_z(\mathcal{B}(K))$, where $K^z(x,y) = z^2K(zx)$.

Observe first that, as $K^z * L^z = (K * L)^z$, we must have:

$$\mathcal{B}((K^{*n})^z) = F_z(n\mathcal{B}(K)) = nF_z(\mathcal{B}(K))$$

Thus, $F_z(rb) = rF_z(b)$ when $r > 0$ is, first, integer, then rational and finally an arbitrary real (using the continuity of F). Therefore $F_z(b) = \phi(z)b$ for some real $\phi(z)$.

Now, $\mathcal{B}(K^{zz'}) = \mathcal{B}((K^z)^{z'})$ gives $F_{z'} \circ F_z = F_{zz'}$ so that:

$$\phi(zz') = \phi(z)\phi(z').$$

But this implies that $\phi(z) = z^\lambda$ for some fixed number λ. Thus we have shown that:

$$\mathcal{B}(K^z) = z^\lambda \mathcal{B}(K).$$

We can interpret this as saying that a change of length unit (in K) gives a simple change of blur unit (in $\mathcal{B}(K)$).

2.2.3. Continuity

Recall that the Schwartz space $\mathcal{S}$ [23] is the set of C^∞ real functions over $\mathbb{R}^2$ satisfying:

$$\forall p \geq 0\ \forall \alpha\ \|f\|_{p,\alpha} := \sup_{x\in\mathbb{R}^2} |x|^p \left|\frac{\partial^{|\alpha|} f}{\partial x^\alpha}\right| < \infty$$

where α ranges over nonnegative multi-indices (α_1, α_2) and $|x|$ is the Euclidean norm of x. The Schwartz topology is given by:

$$f_n \to f \text{ in } \mathcal{S} \text{ iff for every } p, \alpha,\ \|f_n - f\|_{p,\alpha} \to 0.$$

Let $\mathcal{K}'$ be a subset of $\mathcal{K} \cap \mathcal{S}$ endowed with some topology. $\mathcal{K}'$ is **admissible** if it contains all Gaussian kernels, if it is stable under convolution:

$$f, g \in \mathcal{K}' \implies f * g \in \mathcal{K}'$$

and if its topology is weaker than that of $\mathcal{S}$:

$$f_n \to f \text{ in } \mathcal{S} \implies f_n \to f \text{ in } \mathcal{K}'$$

2.3. Axioms

We are now ready to state the axioms that we require of a blur measure, which are either the formalization of properties given in Section 1, a consequence of them, or an irrelevant normalization.

(i) **Normalization:** $\mathcal{B}(G_1) = 1$;
(ii) **Additivity:** for all $f, g \in \mathcal{K}$,
$\mathcal{B}(f * g) = \mathcal{B}(f) + \mathcal{B}(g)$;
(iii) **Invariance:** if H is an isometry of the plane,
$\mathcal{B}(f \circ H) = \mathcal{B}(f)$;
(iv) **Scaling:** there is a positive function ϕ such that for each $f \in \mathcal{K}$, $\lambda > 0$:
$\mathcal{B}(f_\lambda) = \phi(\lambda)\mathcal{B}(f)$
where $f_\lambda(x,y) := \lambda f(\lambda x, \lambda y)$;
(v) **Stability:** $\mathcal{B} : \mathcal{K}' \to \mathbb{R}$ is continuous.

Definition 1 *If $\mathcal{B} : \mathcal{K}' \to \mathbb{R}$ satisfies properties (i), (ii), (iii), (iv) and (v) then we say that $\mathcal{B}$ is an* **additive blur measure.**

Observe that property (i) is a trivial normalization.

3. MAIN RESULT

Our main result is the following uniqueness statement:

Theorem 3 *Let $\mathcal{K}'$ be an admissible subset of the Schwartz space $\mathcal{S}$. Define for $f \in \mathcal{K}'$,*

$$\sigma_x^2(f) = \int_{\mathbb{R}^2} x^2 f(x,y)\,dxdy$$

and define $\sigma_y^2(f)$ likewise.

There is a unique additive *blur measure. It is given by:*

$$\mathcal{B}(f) = \frac{1}{2}\left(\sigma_x^2(f) + \sigma_y^2(f)\right)$$

if this is a continuous functional over $\mathcal{K}'$. Otherwise there is no blur measure.

We remark that the above theorem is valid in a wide range of reasonable topologies so it is not tied to a delicate technical choice.

We also observe that there there is no blur measure in any L^p topology for any p. The weakest admissible topology is of course given by the norm:

$$|f| := \int_{\mathbb{R}^2} (x^2+y^2)|f(x,y)|\,dxdy$$

on the obvious Banach space.

Let us stress that the blur measure is defined essentially by its scalar nature (it is a single number) and its invariance (or composition) properties. The only essential assumption which is explicitely related to the usual notions of blur is that the blur of a Gaussian kernel is non-zero.

4. PROOF OF THE MAIN RESULT

This section is devoted to the proof of the Main Theorem above but let us say before a few words about the ideas involved.

Intuitively, the requirement that $\mathcal{B}(K)$ be isotropic and additive essentially says that $\mathcal{B}$ is a linear function of the logarithm of the MTF. This dependence, because of the scale invariance, must be restricted to the zero frequency. The additivity finally implies that it is (proportional to) the variance.

Technically, we have the necessary continuity properties so that we can start from the Gaussian kernels and generalize to arbitrary kernel through a lemma which is just the usual proof of the central limit theorem of Probability Theory.

4.1. Blur measures for gaussian kernels

The additivity property (ii) together with $G_{\alpha^2} * G_{\beta^2} = G_{\alpha^2+\beta^2}$ implies that

$$\mathcal{B}(G_{nt}) = n\mathcal{B}(G_t).$$

$t \mapsto \mathcal{B}(G_t)$ being continuous in $\mathcal{S}$ and therefore in $\mathcal{K}$, this is well-known to imply that $\mathcal{B}(G_t) = c\cdot t$ for some constant c. The normalization (i) implies that $c = 1$. Thus,

$$\mathcal{B}(G_{\sigma^2}) = \sigma^2$$

By invariance (iii) $\mathcal{B}(G_{\alpha^2/2,\beta^2/2}) = \mathcal{B}(G_{\beta^2/2,\alpha^2/2})$, hence using the additivity (ii'):

$$\begin{aligned}
\mathcal{B}(G_{\alpha^2,\beta^2}) &= \mathcal{B}(G_{\alpha^2/2,\beta^2/2} * G_{\alpha^2/2,\beta^2/2}) \\
&= \mathcal{B}(G_{\alpha^2/2,\beta^2/2}) + \mathcal{B}(G_{\alpha^2/2,\beta^2/2}) \\
&= \mathcal{B}(G_{\alpha^2/2,\beta^2/2}) + \mathcal{B}(G_{\beta^2/2,\alpha^2/2}) \\
&= \mathcal{B}(G_{\alpha^2/2,\beta^2/2} * G_{\beta^2/2,\alpha^2/2}) \\
&= \mathcal{B}(G_{(\alpha^2+\beta^2)/2}).
\end{aligned}$$

Finally, we see that for an additive blur measure one must have:

$$\mathcal{B}(G_{\alpha^2,\beta^2}) = \frac{1}{2}(\alpha^2+\beta^2), \tag{2}$$

i.e., $\bar{\rho}(t) = 1$ for all t in the previous result (**??**).

4.2. Reduction of the general case to Gaussian kernels

In this section $\mathcal{B}$ is an arbitrary additive blur measure. We are going to show that $\mathcal{B}(f) = \mathcal{B}(G_{\alpha^2,\beta^2})$ where $\alpha^2 = \sigma_x^2(f)$, $\beta^2 = \sigma_y^2(f)$.

Let $\hat{f} = \mathrm{TF}(f)$ be the Fourier transform of an image $f \in \mathcal{K}$. Observe that $-\frac{\partial^2 \hat{f}}{\partial x^2}(0,0) = \iint x^2 f(x,y)\,dxdy$ and similarly for the other second order derivatives. Note that the centering of the kernel implies that $\partial^2\hat{f}/\partial x\partial y(0,0) = 0$. Let $\hat{B}(\hat{f}) = \mathcal{B}(\mathrm{TF}^{-1}(\hat{f}))$.

The scaling property gives:

$$\hat{B}(\widehat{f_{n^{1/2}}}) = \frac{1}{n}\hat{B}(\hat{f}). \tag{3}$$

As $\hat{f}.\hat{g} = \widehat{f * g}$, the additivity property (i) gives, for any integer $n \geq 0$, $\hat{B}(\hat{f}^n) = n\hat{B}(\hat{f})$. Together with (3), this gives:

$$\hat{B}(\hat{f}) = \hat{B}\left(\left(\widehat{f_{n^{1/2}}}\right)^n\right).$$

Claim. Setting $\hat{g}(\omega_x,\omega_y) = e^{-\alpha^2\omega_x^2/2-\beta^2\omega_y^2/2}$, we have, for all integers $p \geq 0$ and multi-index α,

$$\|(\widehat{f_{n^{1/2}}})^n - \hat{g}\|_{p,\alpha} \to 0 \qquad \text{as } n \to \infty.$$

This will show that $f_{n^{1/2}}^{*n} \to g$ in $\mathcal{S}$, hence in $\mathcal{K}'$ whose topology is assumed weaker.

Remark. The proof of this claim will be essentially that of the Central Limit Theorem [24].

Before proving the claim, note that it implies the theorem. Indeed, the continuity of $\mathcal{B}$ in $\mathcal{K}'$ implies $\mathcal{B}(f) = \mathcal{B}(g)$ and the conclusions of the theorem follow from the previous analysis of the blur measures for Gaussian kernels.

The first step in the proof of the claim is to observe that

$$\hat{F}_n(x,y) := \widehat{f_{n^{1/2}}}(x,y)^n = \hat{f}(x/n^{1/2}, y/n^{1/2})^n.$$

Write

$$\Delta_t := \{x \in \mathbb{R}^2 : |x| \leq tn^{1/2}\}.$$

and let $\epsilon > 0$ be arbitrarily small.

Recall that the semi-norm that we have to bound is:

$$\sup |x|^p |\partial^\alpha (\hat{F}_n - \hat{g})|.$$

Let $0 < s < 1/2$ be a parameter to be specified latter.

Bound over $\Delta_{\delta n^{1/2}} \Delta_{\delta n^s}$

An easy induction shows that the rth derivative of $\hat{F}_n$ is a sum of terms of the form

$$n^{k/2} \hat{f}'(x/n^{1/2})^\ell \hat{f}^{(i_1)}(x/n^{1/2}) \dots \hat{f}^{(i_p)}(x/n^{1/2}) \hat{F}_{n-i}(x)$$

with $\ell \geq k$ and $0 \leq i \leq r$.

Observe that $|\hat{f}'(x/n^{1/2})| \leq C|x|/n^{1/2}$ for some constant C as $\hat{f}'(0) = 0$ and $\hat{f}$ is smooth. Each derivative of $\hat{f}$ is in the Schwartz space and therefore bounded by a constant times $(1+|x|^2)^q$ for some $q < \infty$. Thus each term above is bounded in absolute value by

$$C(r) \cdot n^{-(\ell-k)/2} |x|^{C(r)} |\hat{F}_{n-i}(x)|.$$

where $C(r)$ is some constant, which we shall increase several times, in the sequel, as necessary.

By assumption, δ being small, there is some $\eta > 0$, such that

$$|\hat{f}(x)| \leq e^{-\eta x^2}$$

for $|x| \leq \delta n^{1/2}$. Therefore, for $n \geq 2r$,

$$\sup_{\Delta_{\delta n^{1/2}} \setminus \Delta_{\delta n^s}} (1+|x|^2)^p |\partial^r \hat{F}_n(x)|$$

$$\begin{aligned} &\leq (1+\delta^2 n)^p \times C(r) \cdot n^{C(r)} \times e^{-\eta(\delta n^s / n^{1/2})^2 \cdot \frac{n}{2}} \\ &\leq C(r) n^{C(r)} e^{-\eta \delta^2 n^{2s}/2} \to 0 \end{aligned}$$

as $n \to \infty$.

Bound over $\mathbb{R}^2 \setminus \Delta_{\delta n^s}$

As $|\hat{f}|$ reaches its maximum value 1 only at 0, there is some $\kappa < 1$ such that

$$|\hat{f}(x/n^{1/2})| \leq \kappa^n$$

for $|x| \geq \delta n^{1/2}$. Thus,

$$\begin{aligned} &\sup_{\mathbb{R}^2 \setminus \Delta_{\delta n^{1/2}}} (1+|x|^2)^p |\partial \hat{F}_n(x)| \\ &\leq \sup_{\mathbb{R}^2 \setminus \Delta_{\delta n^{1/2}}} (1+|x|^2)^p C(r) \cdot n^{-(\ell-k)/2} \max_i |\hat{F}_{n-i}(x)| \\ &\leq \kappa^{n/2} \quad \times C(r) \cdot n^{-(\ell-k)/2} \sup_{\mathbb{R}^2} |x|^{C(r)} |\hat{F}_{n-i}(x)| \\ &\leq \kappa^{n/2} n^{C(r)} \quad \|\hat{f}\|_{C(r),0} \to 0 \end{aligned}$$

as $n \to \infty$.

Bound over $\Delta_{\delta n^s}$

Let $\phi_r(x) = \partial^r g(x)/g(x)$. One shows by induction that

$$\partial^r \hat{F}_n(x) = \left(\phi_r(x) + \sum_{i=1}^{N_r} \frac{x^{q_{ir}}}{n^{k_{ir}/2}} h_r(x/n^{1/2}) \right) \hat{F}_n(x)$$

where $N_r < \infty$, $q_{ir} \geq 0$ and $k_{ir} \geq 1$ are integers and h_{ir} are smooth functions.

The first $\phi_r(x)$ above is taken care of by the following remark:

$$\begin{aligned} |\phi_r(x)\hat{F}_n(x) - \partial^r g(x)| &= |\phi_r(x)(\hat{F}_n(x) - g(x))| \\ &\leq C|x|^p |\hat{F}_n(x) - g(x)| \leq C\|\hat{F}_n - g\|_{p,0} \to 0. \end{aligned}$$

The remaining terms above are bounded by:

$$C(r) \frac{(1+|x|)^{C(r)}}{n^{1/2 - \max(q_{ir})s}} |\hat{F}_n(x)| \leq \frac{C(r)}{n^{1/2-\max(q_{ir})s}}$$

Hence, it is enough to take $s = s(r)$ small enough.

The claim and therefore the theorem are proved.

5. BLUR AND LOW FREQUENCIES

One of the striking implications of our result, is that blur is a **low frequency** phenomenon. To check this, we have taken a natural image and a text image and applied the following various kernels, writing $x = \omega/\omega_{\max}$ with $\omega_{\max}$ the maximum frequency:

1. the usual Gaussian kernel, the multiplication by e^{-16x^2} in Fourier space.

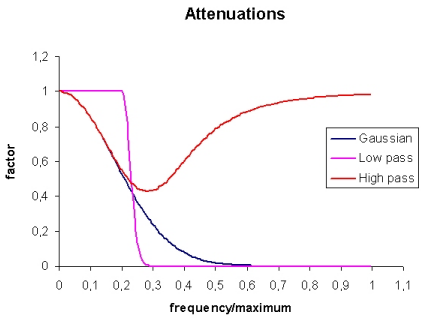

Fig. 5. Profiles of attenuation used in experiments.

2. a cut-off removing all frequencies higher than $\omega_{\max}/5$. This is multiplication by $e^{-256(x-1/5)^{+2}}$.

3. a high-pass filter which removes low frequencies. This is multiplication in Fourier space by $e^{-4x^2/(1+10^3x^8)}$.

The profiles of these kernels are given in Figure 5. The values of the coefficients have been chosen so that the impacts on the L^2 norm are comparable.

The resulting images are given at the end of the paper in Figure 15 and following. In line with the previous experiments, we observe that :

- a strong blur appears after the removal the **low frequencies**, even when the high frequencies were preserved;
- the two images with Gaussian filter and high pass filter have nearly identical perceptual blur;
- the removal of high frequencies, if it introduces a lot of defects (ringing is most visible), does **not** produce perceptual blurring.

6. PERCEPTUAL STUDY

To make the previous observations more systematical, we have selected a collection of natural images and applied several filters to them and asked six subjects to rank them according to perceptual blur. The images were observed at resolution 1:1, on the same CRT display, in the same viewing conditions (distance, illumination, etc.).

The filters were as above:

- none;
- gaussian;
- high pass;
- low pass.

The following gives the average rank of each version of each picture and the average for each processing. One sees that the images are divided into two groups: on the one hand, we have the original image and the low-pass filtered one; on the other hand, we have the images obtained by the Gaussian and high pass filters. Thus the main effect is, as expected, the filtering of low frequencies and the filtering of high frequencies has only a marginal impact.

	original	low pass	high pass	Gaussian
Image 1	1.7	1.3	3.7	3.3
Image 2	1.0	2.0	3.3	3.7
Image 3	2.0	1.3	3.7	3.0
Image 4	1.0	2.0	3.3	3.7
Image 5	1.0	2.0	3.0	4.0
Average	1.3	1.7	3.4	3.6

7. PERFORMING THE MEASURING

We first describe some issues for the implementation of the blur measure.

7.1. Estimating the blur

Recall that the blur of the imaging chain is the (usually small) *difference* between the estimated variance of the input and output images[4]. We have computed directly this evolution of the variance of position in several images after repeated convolution with blurring kernels. We have observed that numerical round-off errors can affect adversely these direct estimations, calling for more sophisticated procedures which we do not discuss here. On the other hand, when the kernel f of the imaging chain has been estimated from other sources, it is easy to measure the blur by computing $\frac{1}{2}\left(\frac{\partial^2 \log \hat{f}}{\partial x^2} + \frac{\partial^2 \log \hat{f}}{\partial y^2}\right)$ at $(x, y) = (0, 0)$. The *DxO Analyzer* of DO Labs implements this idea and the resulting measure is called the **BxU** of the image.

7.2. Normalizing the BxU

Another important issue in the application of the blur measure is its normalization. The blur measure has the dimension of a surface. We note that to be able to compare different imaging chains it is convenient to normalize the blur measure by declaring that the image has a standard size, e.g., $24 \times 36mm^2 = 864mm^2$: one therefore multiplies the blur measure in squared pixels by $864/N$, if N is the number of pixels in the output of the imaging chain. The

[4]The variance of a single image *per se* depends on its content and does not measure blur.

resulting blur is in squared millimiters. It may also be necessary to crop the images if the fields are different.

7.3. Prints of given size of a given scene

Let us give an example of a comparison for a 200 mm x 300 mm print of the same scene taken by two cameras. We consider two Canon cameras: the 1DS and the 300D, using the same 17-40mm f/4-L USM mm Canon lense, focal length 17 mm and aperture 2.8. Sharpening is off for the 1DS and set to normal for the 300D. The blur is measured at the center of the image field:

Cam.	BxU RAW	pixels x 10^6	field %	BxU 200x300mm x 10^{-3}	BxU Corr. x 10^{-3}
1DS	1.26	11	100%	6.9	17.5
300D	1.74	6	40%	17.4	17.4

Table 2. BxU for two cameras: in raw pixels^2, in mm^2 for 200×300 prints (of the full field of each camera), in mm^2 for 200×300 prints of crops to same field.

The lower raw value of the blur for 1DS camera shows that it gives natively a slightly sharper picture than the 300D camera when viewed 1:1 on a given screen.

What happens now if one looks at the pictures when printed on a 200mmx300mm format ? We then have to normalized the BxU accordingly. Since 300D pictures have less pixels than the ones produced by the 1DS, the zoom factor, to achieve this format, will be larger for the 300D. This results in a BxU for the 300D picture which is now almost 3 more times bigger than for the 1DS picture. Since both cameras use the same lens, one can ask: where does this difference of sharpness come from?

The sensors in the 1DS and 300D do not have the same size. They do not cover the same field. The 1DS has a full field sensor (24mm x36mm) where the field of the 300D is around 40% of the 24mm x36mm. Now, let us crop the 1DS picture to the part corresponding to the field of the 300D and then resize this to a 200mm x300mm format. The two 200mm x300mm prints now correspond to the same scene. The BxU of the the 1DS print has to be normalized by multiplying the raw BxU by $200\text{x}300/(11.10^6\text{x}40\%)$, which gives a value almost equal to the 300D one. This last normalization allows one to see that these two cameras (using the same optics) in fact have the *same quality* with respect to blur.

Uniform quality across output devices

Suppose that one wants to deliver the same visual quality through a range of output devices. For example, one may wish to limit the visible blur to 1 pixel^2 on a 17-inch computer screen viewed 50 cm away. This screen corresponds to a solid angle of about 0.37 steradians. If the resolution is 1024x768, then the required maximum blur is $5 \cdot 10^{-7}$ sr, the solid angle under which a pixel is viewed.

Now, what is the requirement for producing an equivalent 10x15 cm print made of 1024x768 pixels? Say that such a print will be viewed 40 cm away, occupying a solid angle of about 0.09 sr. Each squared pixel on the print is therefore $1.2 \cdot 10^{-7}$ sr. Thus one can tolerate a blur of up to 4 pixels^2.

Remark. This illustrates the well-known fact that viewing an image on a screen is much more demanding than simply looking at a medium-sized print.

7.4. Blur and diffraction

Diffraction comes into play at small apertures. We assume therefore in the following computation that one can disregard the effect of the lenses and just consider "pin-hole" image formation.

Let us consider a circular aperture of radius a in a thin, perfectly conducting plane and a linearly polarized incident plane wave with electric field $E(x) = E_0 e^{ik_0 \cdot x}$ making an angle α with the normal to the conducting plane. We compute the wave diffracted into a direction making a angle θ with the normal to the conducting plane. Let ϕ be the azimuthal angle of the direction of emission with respect to the line of polarization.

The Smythe-Kirchhoff vectorial approximation is the recommended approximation for optics according to [13]. It gives a power per solid angle unit of (eq. (9.162) of [13], page 443):

$$\frac{dP}{d\Omega} = \underbrace{\frac{cE_0^2}{8\pi}\pi a^2 \cos\alpha}_{\text{normally incident power}} \cdot \cos\alpha \frac{(ka)^2}{4\pi} \times \times (\cos^2\theta + \cos^2\phi \sin^2\theta) \cdot \left| \frac{2J_1(ka\xi)}{ka\xi} \right|^2 \quad (4)$$

where $k = \|k_0\|$ and

$$\xi^2 = \sin^2\theta + \sin^2\alpha - 2\sin\theta\sin\alpha\cos\phi.$$

Natural light being unpolarized, it contains the polarization corresponding to $\phi = 0$ which gives the dominant contribution according to eq. (4). We thus set $\phi = 0$. ξ becomes:

$$\xi = |\sin\theta - \sin\alpha|$$

$|\theta - \alpha|$ must be small because of the very large factor ka in eq. (4).

Assuming that θ is small, we finally obtain, denoting by f the distance between the stop and the image plane,

$\xi = \cos\theta \cdot \frac{r}{f}$ where r is the distance between the geometric image of the incoming plane wave and the considered point. Thus, the image function of a single point is proportional to the Airy function:

$$\mathrm{Ai}\left(\left|\frac{2J_1(\rho)}{\rho}\right|^2\right) \text{ with } \rho = \frac{2\pi a r}{\lambda f} = \frac{2\pi r}{\lambda n}$$

where $n = f/a$ is the usual f-number.

A key remark is that this function is a rapidly decreasing: $\mathrm{Ai}(\rho) \leq 10^{-3} \cdot \mathrm{Ai}(0)$ for $\rho \geq 12.4$ which corresponds to $r \geq 12.4\frac{\lambda n}{2\pi} \approx 22\mu\mathrm{m}$ for $\lambda = 0.5\mu\mathrm{m}$ and $n = 22$. We introduce the corresponding cut-off in our computations as follows. Let $\widehat{\mathrm{Ai}}(\rho) = \mathrm{Ai}(\rho)$ if this value is larger than $10^{-3}\,\mathrm{Ai}(0)$ and zero otherwise. The BxU is then given by:

$$\frac{\int_0^\infty \widehat{\mathrm{Ai}}(\rho)\left(\frac{\lambda n}{2\pi}\right)^3 2\pi\rho^3 d\rho}{\int_0^\infty \widehat{\mathrm{Ai}}(\rho)\frac{\lambda n}{2\pi} 2\pi\rho d\rho} = \frac{\lambda^2 n^2}{4\pi^2}\frac{\int_0^\infty \widehat{\mathrm{Ai}}(\rho)\,\rho^3 d\rho}{\int_0^\infty \widehat{\mathrm{Ai}}(\rho)\,\rho d\rho}$$

$$= 0.21\mu\mathrm{m}^2 \cdot \lambda^2\mathrm{n}^2 = 0.21 \cdot \left(\frac{\lambda\mathrm{n}}{\mathrm{s}}\right)^2 \text{pixel}^2 \quad (5)$$

if pixels have a s^2 area.

n	2.8	4	5.6	8	11	22
Cameraphone	0.06	0.11	0.21	0.43	0.81	3.25
300D	0.01	0.03	0.04	0.10	0.18	0.7
1DS	0.006	0.01	0.01	0.04	0.06	0.31

Table 3. BxU in raw pixels^2 for three cameras with different pixel sizes of 2.8μm, 6μm and 9μm and various aperture number.

Let us remark that the order of magnitude of these results could have been predicted as follows. The central disk of an Airy figure has radius $1.22 \times \lambda \times n$ so one indeed expects to see a 1 pixel^2 blur starting at $N \approx 14$ for a medium quality digital camera.

We see that, whereas in cameraphones diffraction can contribute significantly to blur, this is not the case for high quality digital camera except at very small apertures.

7.5. Blur as a function of aperture, focal length and position

Let us give some examples of assessments performed on optical devices. Figure 6 illustrates the variation of image quality depending on the aperture and focal length. One clearly sees the existence of a preferred, not extreme aperture and focal length. Remark that:

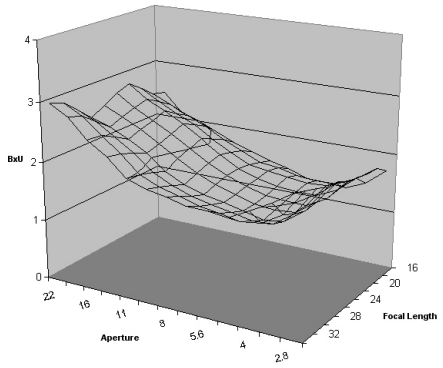

Fig. 6. Blur at the center of the image field of ******, as a function of the lens aperture (A) and focal length (f).

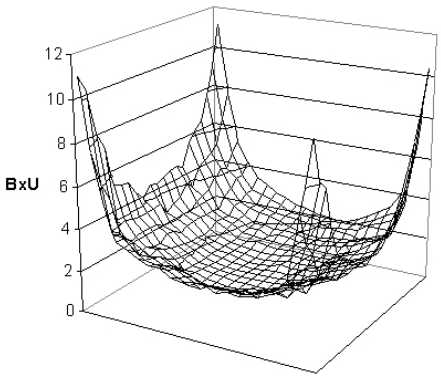

Fig. 7. Blur as a function of position in the image for a Canon 1DS with Canon EF 16-35mm f/2.8L USM, 16 mm focal, aperture 2.8, focused at infinity.

- large apertures present generally more blur, since it is more complex to concentrate light rays away from lenses centers.
- small apertures give rise to diffraction as seen in the previous section.

One can also measure the blur locally, by dividing the image in small subimages. Top quality cameras offer an approximately constant quality throughout the image, see fig. 7 (Canon 1DS with Canon EF 16-35 mm f/2.8L USM).

This degradation in the corner of images is visible in the small detail in Figure 8.

Cameras found in mobile phone have a much variable sharpness, due to obvious constraint of manufacturing:

8. ASSESSING ALGORITHMS

Linear digital processing admit a blur just as well as physical optical chains. We first show the effect of standard blur and sharpening on the blur measure. Then we explain how

Fig. 8. 400x400 bottom left corner of a 4064x2704 image taken with the same material and setting than with the preceding figure. We see a strong increase of blur near the edge, as predicted by the measurements.

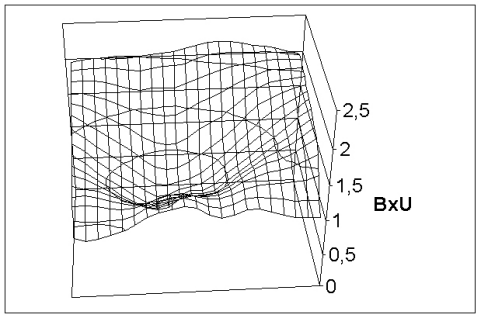

Fig. 9. Blur as a position in the field for a camera embedded in a cell phone.

Fig. 10. Photograph taken with a cell phone.

Fig. 11. A natural image convoluted with larger and larger Gaussian kernels (beginning).

Fig. 12. A natural image convoluted with larger and larger Gaussian kernels (end).

linear zooms can be evaluated from the point of view of blur - here one has to deal with the discrete nature of digital images and the underlying sampling. We then exhibit a linear filter which decreases both the blur and the noise and investigate the theoretical and practical limits of this "optimizing".

8.1. Blur and filtering

We first blur and sharpen some natural images and see how the blur measure correlates to the perceptual quality of the results. The resulting images and blur measures are shown in Figures 11-14.

8.2. Discretized convolutions

We refer to [25] for background on convolution as interpolation. We represent digital images $u_{m,n\in\mathbb{Z}}$ by distributions $u = \sum_{m,n} u_{m,n}\delta_{(m,n)}$. A discretized convolution $\mathcal{L}$ is a map $\mathcal{L} : u \mapsto v$ with

$$v = C_1 \cdot (u * \varphi)$$

where $C_1 = \sum_{m,n} \delta_{(m,n)}$ is the Dirac comb representing the sampling and $\varphi : \mathbb{R}^2 \to \mathbb{R}$ is some kernel. We assume

BxU=3

Fig. 13. A natural image.

BxU=1.3

Fig. 14. The natural image above after a sharpening.

the kernel to be normalized and centered:

$$\sum_{m,n} \varphi(m,n) = 1 \text{ and } \sum_{m,n} m\varphi(m,n) = \sum_{m,n} n\varphi(m,n) = 0.$$

We define the blur of such a transformation to be:

$$\mathcal{B}(\mathcal{L}) := \sum_{n,m} (n^2 + m^2)\varphi(n,m).$$

Thus, $\mathcal{B}(\mathcal{L})$ reflects the "quadratic size" of the spot diagram of $\mathcal{L}$ in the following sense. If σ^2 is the blur of the rendering device (say the quadratic size of the pixels of a screen), then $\mathcal{B}(\mathcal{L}) + \sigma^2$ is the variance of the position in the image generated by $\mathcal{L}$ and the underlying device from an image with just one white pixel. Said differently $\mathcal{B}(\mathcal{L})$ is the increase in blur when the convolution $\mathcal{L}$ is applied before transmitting the image to the given rendering device.

Such a formula is an obvious discretization of our theoretical blur measures. Additivity still holds in this discrete setting:

$$\mathcal{B}(\mathcal{L}_2 \circ \mathcal{L}_2) = \mathcal{B}(\mathcal{L}_1) + \mathcal{B}(\mathcal{L}_2)$$

Indeed, assuming a one-dimensional image for simplicity of notation, the kernel φ_3 of $\mathcal{L}_2 \circ \mathcal{L}_3$ is given by:

$$\varphi_3(n) = \sum_m \varphi_2(m)\varphi_1(n-m)$$

and

$$\begin{aligned}\mathcal{B}(\mathcal{L}_1) + \mathcal{B}(\mathcal{L}_2) &= \sum_{n,m} (m^2 + (n-m)^2)\varphi_2(m)\varphi_1(n-m) \\ &= \sum_{n,m} (n^2 + 2m^2 - 2mn)\varphi_2(m)\varphi_1(n-m)\end{aligned}$$

Using that

$$\sum_m \varphi_i(m-k) = 1, \ \sum_m m\varphi_i(m-k) = k$$

we see:

$$\sum_m m^2\varphi_2(m) \sum_n \varphi_1(n-m) = \sum_m m^2\varphi_2(m)$$

and

$$\sum_m m\varphi_2(m) \sum_n n\varphi_1(n-m) = \sum_m m^2\varphi_2(m)$$

Therefore

$$\mathcal{B}(\mathcal{L}_1) + \mathcal{B}(\mathcal{L}_2) = \sum_{n,m} n^2\varphi_2(m)\varphi_1(n-m) = \mathcal{B}(\mathcal{L}_2 \circ \mathcal{L}_2)$$

This proves additivity.

8.3. Application to linear zooms

We show how the blur measure can be applied to study linear zooms. To keep this illustrative section simple, we shall make some approximations that are valid for large zoom factors (see eq. 6). A definitive study would require doing the discrete computations explicitely.

In the above formalism, a linear zoom of factor $\lambda > 1$ is a map $\mathcal{Z} : u \mapsto v$ with

$$v = C_1 \cdot \Phi_\lambda(u * \varphi)$$

where $\Phi_\lambda(\psi) = \lambda^{-2}\psi(\cdot/\lambda, \cdot/\lambda)$. That is,

$$v_{k,\ell} = \sum_{m,n} \lambda^{-2}\varphi(k/\lambda - m, \ell/\lambda - n)u_{m,n}$$

We again define the blur to be the quadratic size of the corresponding spot diagram:

$$\mathcal{B}(\mathcal{Z}) = \sum_{k,\ell}(k^2 + \ell^2)\lambda^{-2}\varphi(k/\lambda, \ell/\lambda)$$

If λ is large, then

$$\mathcal{B}(\mathcal{Z}) \approx \int (x^2 + y^2)\varphi(x, y)\, dxdy.$$

This notion is approximately additive. Let us prove that $\mathcal{B}(\mathcal{Z} \circ \mathcal{Z}') \approx \mathcal{B}(\mathcal{Z}) + \mathcal{B}(\mathcal{Z}')$ under reasonable hypothesis, eq. (6). Writing $v = \mathcal{Z}'(u)$ and $w = \mathcal{Z}(v)$ and again pretending that there is only one dimension for simplicity,

$$\begin{aligned} w_n &= \sum_m \lambda^{-1}\varphi(n/\lambda - m)v_m \\ &= \sum_{m,k} (\lambda\lambda')^{-1}\varphi(n/\lambda - m)\varphi'(m/\lambda' - k)u_k \\ &= \sum_k (\lambda\lambda')^{-1}\varphi''(n/\lambda\lambda' - k)u_k \end{aligned}$$

with

$$\begin{aligned} \varphi''(n/\lambda\lambda' - k) &= \sum_m \varphi(n/\lambda - m)\varphi'(m/\lambda' - k) \\ &= \sum_{M \in \mathbb{Z}/\lambda'} \varphi(n/\lambda - \lambda' k - \lambda' M)\varphi'(M) \end{aligned}$$

with $M = m/\lambda' - k$. Setting $N = n/\lambda\lambda' - k$, we see that the above equality holds if, for all $N \in \mathbb{Z}/\lambda\lambda'$:

$$\varphi''(N) = \sum_{M \in \mathbb{Z}/\lambda'} \varphi(\lambda'(N - M))\varphi'(M)$$

A computation entirely similar to the one for composition of discretized convolutions proves the claim provided that, for $z = \lambda, \lambda'$, we have the normalization and centering:

$$\sum_{n \in \mathbb{Z}/z} \varphi(n) \approx 1 \text{ and } \sum_{n \in \mathbb{Z}/z} n\varphi(n) \approx 0. \qquad (6)$$

Example

We consider zooms of the above form $\mathcal{Z}_\lambda(f) = C_1 \cdot \Phi_\lambda(u * \varphi)$ for:

1. (piecewise constant) $\varphi(x) = 1_{[-1/2,1/2]}$;
2. (pieceiwse linear) $\varphi(x) = 1_{[-1,1]}(1 - |x|)$;
3. (bicubic) $\varphi(x) = (a + 2)|x|^3 - (a + 3)|x|^2 + 1$ for $|x| < 1$, $a|x|^3 - 5a|x|^2 + 8a|x| - 4a$ for $1 \leq |x| < 2$ and $\varphi(x) = 0$ for $|x| \geq 2$.

For large zoom factors, $\mathcal{B}(\mathcal{Z}_\lambda) \approx 2\int x^2\varphi(x)\, dx$ and we obtain:

1. $1/6$ for the piecewise constant case;
2. 1 for the bilinear case;
3. $(8a + 4)/3$ for the bicubic case. It is zero for $a = -1/2$, the much used bicubic interpolation scheme of Keys [15].

Consider an imaging chain made of a camera with blur σ_1^2 (in squared pixels) and a screen with blur σ_2^2 (in mm^2) so that the resulting blur is

$$\sigma^2 := \kappa(S\sigma_1^2 + \sigma_2^2)$$

in steradian if S is the surface of a pixel on the screen and κ is the solid angle corresponding to a unit of surface on the screen.

We now insert one of the above zooms with blur B and scale factor of λ just before the screen in this same optical chain. The blur of the imaging chain becomes:

$$\sigma_Z^2 := \kappa(\lambda^2 S(\sigma_1^2 + B) + \sigma_2^2)$$

Comparing with a pure rescaling (i.e., a closer look to the same screen) for which the blur would become $\lambda^2\sigma^2$ we have:

$$\sigma_Z^2 = \lambda^2\sigma^2 + \lambda^2\kappa(SB - (1 - \lambda^{-2})\sigma_2^2).$$

We see that

- for the piecewise constant zoom $SB \approx \sigma_2^2$, hence the effect is about the same as looking closer at the screen —we have just "painted" big pixels using the small screen pixels;
- for the bilinear zoom the blur is significantly increased as it is expected;
- for the bicubic zoom only the camera blur is multiplied by λ, but the screen blur stays the same.

One could ask whether a zoom with negative blur would not be even better but it is obvious that blur does not, by itself, capture all the quality of a zoom and misses some defects like blockiness, ringing or saturation. Indeed, a zoom which would just insert black pixels would be best if minimizing blur was the only criterium. Nevertheless, we think that the blur measure has a role to play in a theory of "optimal zooms" as developed in [25].

8.4. Linear filtering of blur and noise

We investigate in this section the relationship between blur and another image defect: **noise**. We consider here additive noise, that is, the observed image is the ideal image plus a random image. The noise level is measured as the variance of the grey level of a pixel of this random image.

One often considers that there is a direct trade-off between reducing noise and reducing blur. It is expected that sharpening will blow up noise and, conversely, that the reduction of noise requires smoothing which inevitably add blur. We prove in this section that things in fact are more complicated. One can indeed decrease both blur and noise by a linear filter. However, another kind of defect will appear, so that it is not clear how to take practical advantage of the previous remark.

8.5. Improving both noise and blur

Consider the following discrete kernel:

$$\begin{pmatrix} c & b & c \\ b & a & b \\ c & b & c \end{pmatrix}$$

We assume that the optical chain is defined by $u \mapsto K * u + n$ where K is a normalized kernel and n is an impulsional noise with grey level random variance σ^2, i.e., an array of i.i.d. random variables with mean 0 and variance σ^2 (to make the analysis easier). The blur added by the optical chain is $\mathcal{B}(K)$, which is $4b + 8c$. A straightforward computation shows that the random variance of the grey levels in the processed image is: $\sigma^2(a^2 + 4b^2 + 4c^2)$.

We assume K to be:

- normalized: $a + 4b + 4c = 1$;
- non bluring: $4b + 8c = 0$;
- noise reducing: $a^2 + 4b^2 + 4c^2$ minimum.

The best choice is therefore:

$$\begin{pmatrix} -1/9 & 2/9 & -1/9 \\ 2/9 & 5/9 & 2/9 \\ -1/9 & 2/9 & -1/9 \end{pmatrix}$$

Fig. 15. A natural image.

It multiplies the noise by $5/9$ without increasing blur (one could obviously decrease the noise a little less and actually decrease the blur).

We present a natural image (Fig. 15) and its "optimized" version obtained by applying four times the above 3x3 filter. One sees that the simultaneous removal of blur and noise has in fact a cost: the image becomes "textured".

9. CONCLUSION

In this paper we have shown that once one writes down a minimum list of reasonable mathematical properties that a useful blur measure of imaging chains should possess, there is a **unique** theoretical solution: the *variance* of the positions in the kernel.

This variance had of course been considered in many related problems, e.g., blind deconvolution or depth estimates from blur (see for instance [20, 16] and the references therein) — or showed to be strongly correlated with other seemingly distant blur assessments both objective and subjective [19]. But our result is independent of any assumption on the blur kernel (which we do not need to estimate and which maybe far from Gaussian). In fact, the main point of this paper is to give a unique coherent extension to arbitrary kernels of the obvious blur measure for Gaussian kernels which are generally assumed in most of the literature.

The uniqueness we obtain offers a potential bridge between our mathematical approach and psychophysical blur. Experiments presented above and the use of the resulting measure[5] by professionals[6] which previously used other,

[5] DXO Analyzer of the DXOLabs company.

[6] Photograph magazines like [7, 18] and mass retailers [10].

Fig. 16. A natural image “optimized”.

more classical tools before have shown that a very meaningful connection does exist.

Our result implies that high frequency attenuation is, contrarily to expectations, irrelevant to the measure of blur and, by the above connections, to perceptual blur. One can remember that human perception is quite insensitive to high frequencies, so that our result should perhaps be less of a surprise. We also remark that our measure has a natural interpretation in terms of the spot diagram: it is the square of the “size” of the spot diagram, as measured by its second order moment.

In this paper, we have shown how this blur measure can be used for the evaluation both of physical optical chains and algorithms. We believe that beyond the simple example we presented above, this blur measure can be used to optimize zooms and other linear algorithms (cf. [3]).

10. REFERENCES

[1] L. Alvarez, F. Guichard, P.-L. Lions, J.-M. Morel, Axioms and fundamental equations of image processing, *Arch. Rational Mech.*, vol. 123, no. 3, 199-257, 1993.

[2] D. Berfanger, N. George, All-Digital Ring Wedge Detector Applied to Image Quality Assessment, *Applied Optics*, Vol. 39, no. 23, 4080-4097, August 2000

[3] T.Blu, M.Unser, Quantitative Fourier Analysis of Approximation Techniques: Part I—Interpolators and Projectors, Part II—Wavelets, *IEEE Trans. Signal Process.*, **47** (1999), no. 10, 2783–2806.

[4] M. Born, E. Wolf, *Principles of Optics: Electromagnetic Theory of Propagation, Interference and Diffraction of Light*, Cambridge University Press, 1999.

[5] A. Bovik, *Handbook of image & video processing*, Academic Press, 2000.

[6] J. Buzzi, F. Guichard, *Uniqueness of blur measure*, IEEE International Conference on Image Processing, Singapore, 2004.

[7] *Chasseur d’images*, march 2004 issue.

[8] M. Chiang, T. Boult, Local blur estimation and superresolution, *Proc. IEEE conference on computer vision and pattern recognition*, 1997, pp. 821.

[9] J. Dijk, M. van Ginkel, R. van Asselt, L. van Vliet, P. Verbeek, A new sharpness measure based on Gaussian lines and edges, in: N. Petkov, M.A. Westenberg (eds.), *Computer Analysis of Images and Patterns - CAIP 2003 (Proc. 10th Int. Conf., Groningen, NL, Aug.25-27)*, Lecture Notes in Computer Science, vol. 2756, Springer Verlag, Berlin, 2003, 149-156.

[10] FNAC, *Les appareils photo numériques*, summer 2004.

[11] L. Florack, *Image Structure*, (Computational Imaging and Vision, vol. 10), Kluwer Academic Publishers, 1997.

[12] L. Florack, B. Romeny, J. Koenderink, M. Viergever, Scale and the differential structure of images, *Image and Vision Computing* **10**, no. 6, 376 - 388, July/Aug. 1992

[13] J.D. Jackson, *Classical electrodynamics, Second Edition*, Wiley & sons, 1975.

[14] V. Kayargadde, J.-B. Martens, Perceptual characterization of images degraded by blur and noise: experiments, *J. Opt. Soc. Am.*, Series A, vol. 13, no. 6, June 1996.

[15] R. G. Keys, Cubic convolution interpolation for digital image processing. *IEEE Trans. Acoustics, Speech, and Signal Processing*, **29**, no. 6, 1153-1160, Dec. 1981.

[16] D. Kundur, D. Hatzinakos, Blind image deconvolution, *IEEE Signal Processing Magazine*,, **13** (1996), 43–64.

[17] R. Lagendijk, J. Biemond, Basic methods for image restoration and identification, in *Handbook of image and video processing*, A. Bovik (editor), Academic Press, 2000.

[18] The luminous landscape, l `http://www.luminous-landscape.com`, 2004.

[19] P. Marziliano, F. Dufaux, S. Winkler, and T. Ebrahimi, A No-Reference Perceptual Blur Metric, *Proc. International Conference on Image Processing*, Rochester, NY, Sept. 22-25, 2002.

[20] P. Favaro, A. Mennucci, S. Soatto, Observing shape from defocused images, *Internat. J. Computer Vision* **52** (2003), 25–43.

[21] ISO12233, `http://www.iso.ch`.

[22] S. Ray, *Applied photographic optics*, 3rd edition, Focal Press, 2002.

[23] W. Rudin, *Functional analysis, 2nd edition*, McGraw-Hill, 1991.

[24] D. Stroock, *Probability Theory, an Analytic View*, Cambridge University Press, 1994.

[25] P. Thévenaz, T. Blu, M. Unser, Interpolation revisited, IEEE Transactions on Medical Imaging, vol. 19, no. 7, pp. 739-758, 2000

[26] M. Unser, A. Aldroubi, M. Eden, Enlargement or reduction of digital images with minimum loss of information, *IEEE Trans. Image Process* **4** (1995), 247–258.

[27] Z. Wang, A. Bovik, H. Sheikh, E. Simoncelli, Image quality assessment: from error visibility to structural similarity, *IEEE Trans. Image Processing*, vol. 13, no. 4, April 2004.

[28] Z. Wang, E. Simoncelli, Local Phase Coherence and the Perception of Blur, in *Advances in Neural Information Processing Systems* **16** (2004), eds. S. Thrun, L. Saul, B. Schlkopf, MIT Press.

[29] J. Weickert, *Anisotropic Diffusion in Image Processing*, ECMI Series, Teubner, Stuttgart, 1998.

[30] D. Williams, What is MTF and why should you care, *RLG Diginews*, **2**, no. 1, February 1998.

Fig. 17. A natural image.

Fig. 19. Natural image with low pass filter.

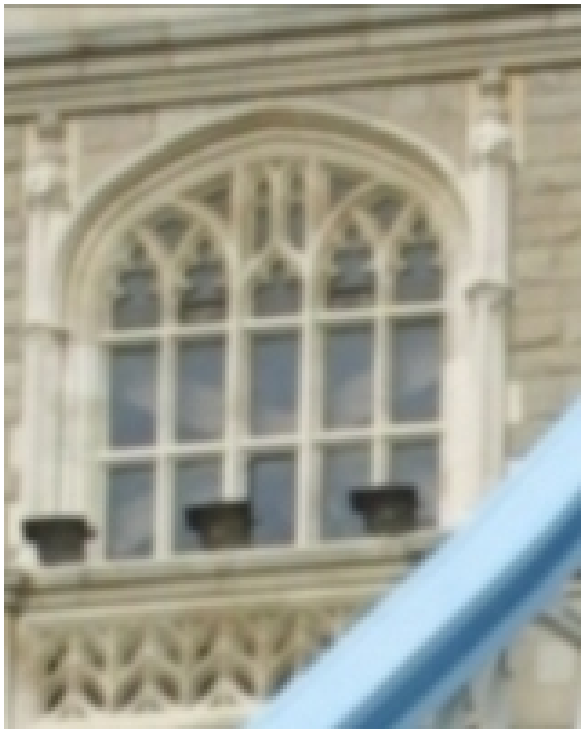

Fig. 18. Natural image convoluted with a Gaussian kernel.

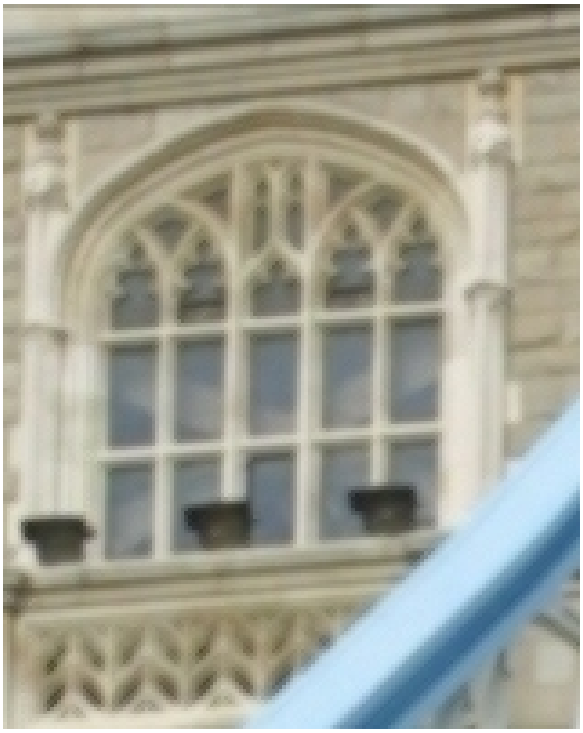

Fig. 20. Natural image with high pass filter.